Taguchi method optimization of wax production from pyrolysis of waste polypropylene

A green nanotechnology approach

**Neeraj Mishra · Niranjan Patra · Sunil Pandey ·
Marco Salerno · Madhuri Sharon · Maheshwar Sharon**

Abstract Present research deals with the conversion of
waste commodity plastics to valuable commercial product
in the form of wax by pyrolysis. Optimization of both
processes yield and produced wax quality was performed
by means of a statistical tool originally proposed by
G. Taguchi, using temperature, catalyst, carrier gas, and
dwell time as the parameters. The obtained wax was
characterized by Raman spectroscopy, differential scan-
ning calorimetry, and thermogravimetric analysis. Yield of
wax was found to be maximum when the parameters were
600 °C, Fe catalyst, nitrogen gas atmosphere, and 15 min
time. However, stability of the wax was found to be opti-
mum at 700 °C. Calorific value of the wax thus obtained
was ~ 43 MJ kg^{-1}, which supports its suitability as fuels
like other petroleum products.

Keywords Wax · Taguchi optimization method ·
Calorific value · Waste plastics recycling

Introduction

In less than a century, plastics have become exceptionally
user friendly, moving from almost no presence at all to near

N. Mishra (✉) · S. Pandey · M. Sharon · M. Sharon
N. S. N. Research Centre for Nanotechnology &
Bionanotechnology, Ambernath (W), Maharashtra, India
e-mail: mishraneerajprakash@gmail.com

N. Patra · M. Salerno
Department of Nanophysics, Istituto Italiano di Tecnologia, Via
Morego 30, 16163 Genoa, Italy

ubiquity. One of the most widespread plastics is polypro-
pylene (PP), which is used in approximately 40 % of total
packaging and carrying containers worldwide, correspond-
ing to over 1 million PP plastic bags consumed per minute
[1]. Whereas in recent years the local regulations of the
western countries forced the commercial distribution to use
biodegradable plastics based on biopolymers such as e.g.,
starch [2], in the emerging countries, the over exploitation
of PP bags is still going on and creates potential environ-
mental and human health risks [3]. Therefore, intensive uses
of traditional non-biodegradable plastics demand a robust
and eco-friendly route to recycle and utilize properly the
plastic wastes. Normally, plastics can be used as carbon
precursors for synthesis of carbon nanotubes (CNTs), wax,
oil and gases, providing at the same time the opportunity for
production of valuable goods and for disposal of large
amounts of plastic waste. In terms of energy reutilization, to
convert polyolefins to valuable product seems a better
option than direct consumption of ethane, propane, and
other compounds from petroleum source.

The pyrolysis technique can potentially be used to
convert waste plastics into valuable products like fuel [4],
carbon materials [5], and chemicals [6]. We have already
discussed synthesis of CNTs [5] and crude oil [7] using
pyrolysis technique in earlier publications. Since current
market is high in demand for manufacture of wax, in this
work we have used pyrolysis for the synthesis of wax.
Several technologies have been applied in both thermal and
catalytic pyrolysis of waste plastics, such as fixed beds [8],
rotator conical reactor [9], pyrolysis chemical in molten
salts [10], and circulating sphere reactor [11–13], but cat-
alytic pyrolysis reactor is the more widely studied tech-
nology at laboratory as well as in pilot plant scale [14].
Aguado [15] has synthesized wax from thermal pyrolysis
of PP and high density polyethylene (HDPE) in a conical

spouted bed reactor (CSBR) at a temperature of 400-600 °C, with process efficiency of 92 mass%. Elordi [16] has synthesized wax at 500 °C using a spent fluidized catalytic cracking (FCC) catalyst agglomerated with bentonite (50 mass%) in a CSBR, showing efficiency of 67 mass%. A low molecular mass PE wax was prepared from PE by Umare [17] using titanium BINOLate-ethylaluminum sesquichloride catalyst system. Li [18] has also synthesized PE wax from waste PE, with a process yield of over 90 %.

In most cases cited above, the technical protocols used are cumbersome, and the involved procedures are tedious and cost expensive. Most PP wax is made from the pyrolysis of PP resin, or virgin polymer, so its cost is high, and the world market is in short supply. Also, wax is a sticky material and is difficult to take out from a reactor like CSBR and FCC. We have explored a novel method to convert waste PP into commercially viable wax [19]. In our process we can use any form or shape of plastic in the reactor in large quantity, which makes insertion of plastic waste and collection of product handy. Vapor condenses at the end of horizontal stainless steel tube furnace, i.e., the cooler region, which helps for product collection and prevents from mixing it with other products.

Another significant advancement of this work is the use of the statistical method invented by Taguchi [20, 21] in order to reduce the number of experiments involved in process optimization. We have selected four independent process parameters for the synthesis of wax, and each of them has three different possible values. Hence, in order to obtain a full characterization, one would be required to carry out all factorial design combinations of 3^4 i.e., 81 experiments. However, Taguchi optimization methodology helps in reducing the number of experiments, obtaining similar and in principle equivalent information, by some approximation. In our case, this allowed to perform only nine sets of experiments out of the whole set of 81 required by a full factorial design.

The influence of the reaction temperature on the thermal stability and composition of condensed product have been investigated by thermogravimetric (TG) analysis and differential scanning calorimetry (DSC) in nitrogen (N_2) atmosphere. The resulting stability is different for the wax formed at different temperatures. It is therefore clear that the thermal stability and yield strongly depend on the processing conditions.

Materials and methods

Starting materials

Analytical grade nickel nitrate, cobalt nitrate, and ferric nitrate were purchased from SD fine chemicals, India, and used as received. Urea was purchased from Finar chemicals, India, and used as received. Waste PP was collected from Kalyan-Dombivali Municipal Corporation (KDMC) garbage center, Kalyan, MS, India. Prior to use, the waste PP was washed with detergent for two to three times and dried in open air/sunlight.
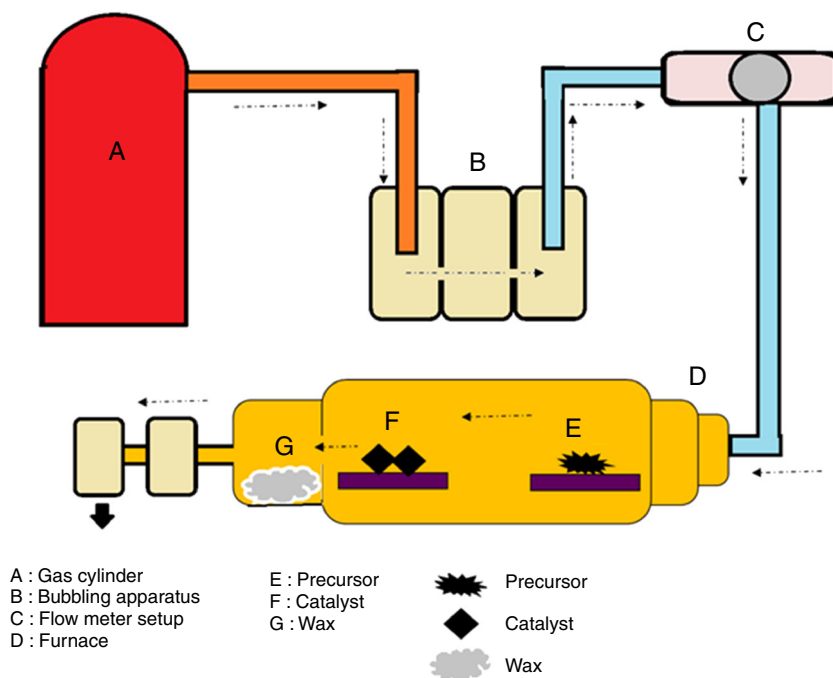
Pyrolysis of the waste PP

Pyrolysis of waste PP was conducted as per the parameters shown in Taguchi table (Table 1). An orthogonal table was constructed using three levels of each parameter. Mass of synthesized materials was used for the calculation of signal to noise (S/N) ratio, where the larger value the better (see Eq. 1). Each level was repeated three times for the reproducibility of result and took the average of three values i.e., mass (yield) of wax to convert into single value to calculate the S/N ratio. Since the selection of the parameter values corresponding to the combinations (i.e., levels) listed in Table 1 is used as an experimental process guide but is also the result of Taguchi optimization, details of this processing are presented in "Taguchi optimization and effect of parameters on wax" section. In each experiment, 10 g of the material was loaded in the center of a horizontal tube furnace of $100 \times 19 \times 12.5$ cm^3 size made in stainless steel 316 grade, with 0.1 g catalyst (Fe, Ni or Co), placed in another quartz boat with respect to the PP (see Fig. 1). Catalyst was prepared from Ni/Fe/Co nitrate salt by urea decomposition method [22]. The furnace was equipped with condenser to cool the exit gases before they are allowed to escape, and the product of condensation was collected in a flask attached to it. The purpose of the condenser is to increase the yield of wax product. PP hydrocarbons have different fractions of C atoms, and at the high temperature they are found in vapor state. Some of the lower-fraction C atoms (C1-C3) are difficult to condense, but our aim was to condense the maximum amount of vapor from hydrocarbon fractions like C20-C70. 100 sccm of Ar/H_2/N_2 gas was used to make the furnace atmosphere oxygen free. Temperature (600, 700, and 800 °C) and duration of pyrolysis (5, 10, and 15 min) were set at desired value by digital temperature controller. After the desired time interval had elapsed, the furnace was cooled down, and the obtained product was collected.

Characterization techniques

Raman spectra of the formed wax were acquired at room temperature upon irradiating a spot of ∼2 μm diameter on the specimen with ∼1 mW power of an incident diode–pumped solid state laser at $\lambda = 632.8$ nm wavelength, coupled into an optical microscope with a 50× objective lens. The Raman scattered radiation was collected between

Table 1 Arrangement of L9 orthogonal parameters as per Taguchi optimization technique, with respective S/N ratio, resulting yield of wax formation, and additional quantities required to determine the importance of difference parameters in optimizing the yield

Level	Temperature/ °C			Catalyst			Gas			Duration/min			Wax yield/ %
	600	700	800	Fe	Ni	Co	Ar	H_2	N_2	5	10	15	(mean ± SD)
L-1	18.10			18.10			18.10			18.10			80.4 ± 9.48
L-2	18.46				18.46			18.46			18.46		83.8 ± 10.45
L-3	17.60					17.60			17.60			17.60	75.9 ± 10.87
L-4		17.58		17.58				17.58				17.58	75.7 ± 10.66
L-5		17.37			17.37				17.37	17.37			73.9 ± 11.57
L-6		7.42				7.42	7.42				7.42		23.5 ± 10.30
L-7			16.95	16.95					16.95		16.95		70.4 ± 8.18
L-8			15.74		15.74		15.74					15.74	61.3 ± 10.57
L-9			10.34			10.34		10.34		10.34			32.9 ± 7.35
S/N sum	54.16	42.37	43.03	52.63	51.57	35.36	41.26	46.38	51.92	45.81	42.83	50.92	(Avg: 46.52)
Deviation S/N	7.64	−4.15	−3.49	6.11	5.05	−11.1	−5.26	−0.14	5.40	−0.71	−3.69	4.40	
m_{ij}	18.05	14.12	14.34	17.54	17.19	11.79	13.75	15.46	17.31	15.27	14.28	16.97	–
$<m_i>$	15.51			15.51			15.51			15.51			–
SOS_i	29.26			62.46			18.95			11.10			–
FOE_i	24.02			51.27			15.55			9.16			–

Fig. 1 Schematic diagram of the pyrolysis setup

A : Gas cylinder
B : Bubbling apparatus
C : Flow meter setup
D : Furnace

E : Precursor
F : Catalyst
G : Wax

Precursor
Catalyst
Wax

500 and 3,500 cm^{-1} by the same objective and analyzed by a LabRam HR spectrometer (Horiba Jobin–Yvon, Italy) with a resolution of 4 cm^{-1}. Typical acquisition times were on the order of 20 s. All the spectra were baseline corrected and were normalized thereafter.

The DSC measurements were carried out on a Pyris Diamond SII instrument (Perkin-Elmer, Waltham, MA, USA), repeatedly scanning the temperature upward and then downward between 0 and 100 °C at a rate of 10 °C min^{-1}, under N_2 atmosphere with a flow rate of 20 mL min^{-1}. Thermal behavior like melting and crystallization temperatures and enthalpies were determined from the second scan. The DSC instrument was calibrated using Indium as the standard reference material. The amount of sample was approximately 10 mg in all the DSC measurements.

TG measurements were carried out on Q500 (TA Instruments, New Castle, DE, USA), scanning the temperature from 30 to 600 °C at a rate of 10 °C min^{-1}, under N$_2$ atmosphere with a flow rate of 20 mL min^{-1}. The amount of sample was ∼10 mg in all TG measurements.

Calorific value of wax was determined using PARR isoperibolic oxygen bomb calorimeter 1138 (Parr Instruments, Moline, IL, USA) under cooling with jacket having 2 L of water. The amount of wax introduced into the system for its combustion was ∼1 g.

Results and discussion

Taguchi optimization and effect of parameters on wax

Orthogonal array yield and S/N ratio values of various experiments are shown in Table 1. All the nine samples were synthesized with the same procedure as mentioned above. From the yield, S/N ratio for wax was calculated by using following equation, for larger the better [19]:

$$\frac{S}{N} = -10 \log 10 \left[1/n \sum 1/y^2 \right] \quad (1)$$

where y is the primary response and n is the number of repetitions of each experiment. From the graphical display of the deviation of S/N ratio sums (Fig. 2a), positive and negative effects of different levels on yield of the product can be seen. Positive values of the sums indicate dominance of the parameter on the yield, as well as on the quality of the wax. The most ideal parameters as deduced from Fig. 2a were found to be 600 °C pyrolysis temperature, Fe as catalyst, 15 min of dwell time, and N$_2$ as the carrier gas. In this case the wax was found to be soft and yellow in color. The corresponding yield obtained was around 80 mass% (with standard deviation of the three measurements σ ∼ 10 % of mean value, see Table 1). Obviously, an increase in pyrolysis temperature leads to decrease in wax yield. One of the reasons for decrease in wax is conversion of wax to gaseous products at high temperature, which are lost through the flow of carrier gas [4, 16, 18]. Also, at 600 °C, plastic gets melted completely (vapor form) and comes into contact with the catalyst, which leads to vigorous gas-solid reaction and avoids the formation of secondary reactions that results into formation of additional wax [7, 10]. It is known that thermal degradation occurs by a free-radical mechanism, and it offers many oligomers by hydrogen transfer from the tertiary carbon atom to the radical site along the polymer chain. However, catalytic degradation of PP is known to proceed by carbonation mechanism [1, 23, 24]. The initial step of the degradation reaction is considered to occur by either the abstraction of the hydride ion H$^+$ (by Lewis acid theory)
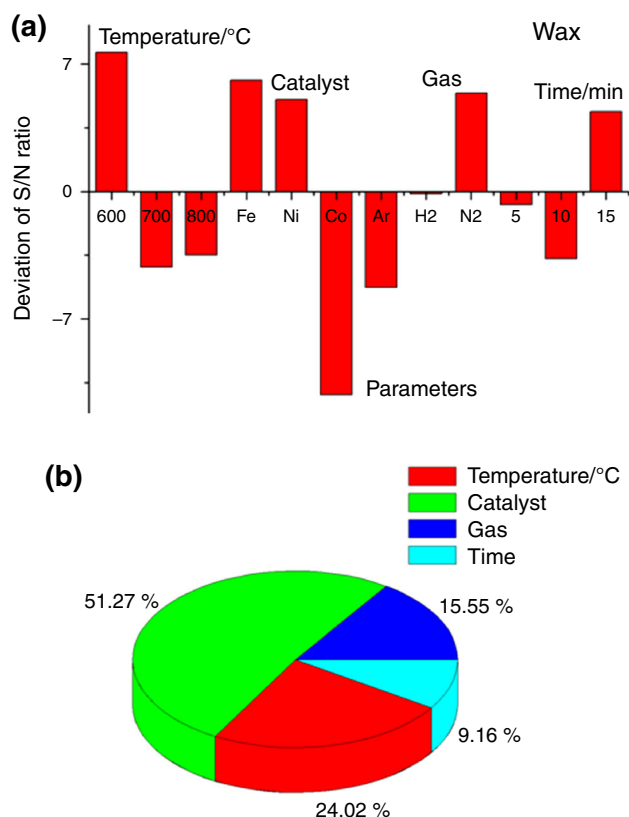

Fig. 2 a Plot of deviation of S/N ratio of different Taguchi levels from Table 1 (S/N sum—S/N overall average); **b** Pie-chart showing the relative importance of the different parameters in determining the maximum yield, as determined by full Taguchi calculations

from the PP molecule or by the addition of a proton (by Broensted acid theory) to the C-C bonds of the PP molecule or thermally degraded olefins. Therefore, it can be concluded that Fe or Ni catalyst with moderate temperature of 600 °C accelerated the cracking of light hydrocarbon fragments but inhibited the aromatization of naphthalene by activating hydrogen to react with aromatics. Nickel is commonly used for the hydrogenation of aromatics to aliphatic compounds, which can be one reason for the inhibition of aromatization [24].

Park [25] has explained the effect of contact time, where longer contact time promotes primary cracking products and minimizes secondary reaction, which results in an increase in the yield of liquid wax formation that becomes solid after cooling. In short contact time, the distribution of carbon numbers also shifted to lower values [26]. The gas used during the experiment has valuable role for making the atmosphere air or oxygen-free in the pyrolysis system.

In addition to finding the conditions for highest wax yield, we also wanted to determine the relative importance of each considered parameter in reaching this result. To this goal, we first calculated the average S/N sum value for each column, called m_{ij}, for $i = 1$-4 corresponding to the

four different parameters and $j = 1$–3 corresponding to the three different values of each parameter considered in Table 1. Then, for $i = 1$–4, we averaged among the three columns, finding the average value $<m_i>$ for each parameter, $i = 1$–4. Therefore, the equations used to calculate the above quantities were [19]

$$m_{ij} = \left(\frac{1}{N_i}\right) \sum_{\text{incolumn}} \frac{S}{N} \quad \text{with } N_i = 3 \quad \text{for all } i = 1 \text{ to } 4 \tag{2}$$

$$\langle m_i \rangle = \left(\frac{1}{N_j}\right) \sum_j m_{ij} \quad \text{with } N_j = 3 \quad \text{for all } j = 1 \text{ to } 3 \tag{3}$$

Accordingly, the sums of squares (SOS) for each parameter were also calculated as [19]

$$\text{SOS}_i = \sum_j {}_i (m_{ij} - \langle m_i \rangle)^2 \tag{4}$$

Then, considering a number of degrees of freedom (DOF) equal to number of parameter levels -1, i.e., DOF $= 3\text{-}1 = 2$, the so-called factor of effects (FOE) were finally calculated, according to [19]

$$\text{FOE}_i = \frac{\text{SOS}_i}{\text{DOF} \times \sum_j \left(\text{SOS}_j / \text{DOF}\right)} \tag{5}$$

These FOE_i values represent the percentage influence of the respective i parameter on the obtained Taguchi optimized result of the process. As such, they were plotted in Fig. 2b. One can see that, among all the four parameters, the most influential one for optimization of wax yield was the type of catalyst ($\sim$51 %), next was the temperature ($\sim$24 %), and third was the type of gas ($\sim$16 %), whereas duration of the process was the least important ($\sim$9 %).

Until now, we have discussed the parameters for maximizing the yield of wax, but the stability of wax is also a pivotal parameter to be discussed. To this goal, we synthesized wax at three different temperatures of 600, 700, and 800 °C using Fe as catalyst, for a dwell time of 15 min and in the N_2 atmosphere.

Raman scattering

Raman spectra of the three wax samples are shown in Fig. 3. Most peaks in these traces have been interpreted in previous works [15, 27, 28], and the respective assignments have been reported by appropriate labeling in Fig. 3 (for a whole description see Table S1). In particular, the strong bands at 2875 and 2888 cm^{-1} are assigned to symmetric and asymmetric CH_2 stretching, respectively [29, 30], while the symmetric and asymmetric CH_3 stretching causes the two shoulders at 2961 and 2929 cm^{-1}, respectively [30]. Another important feature is the olefinic band at 3080 cm^{-1},
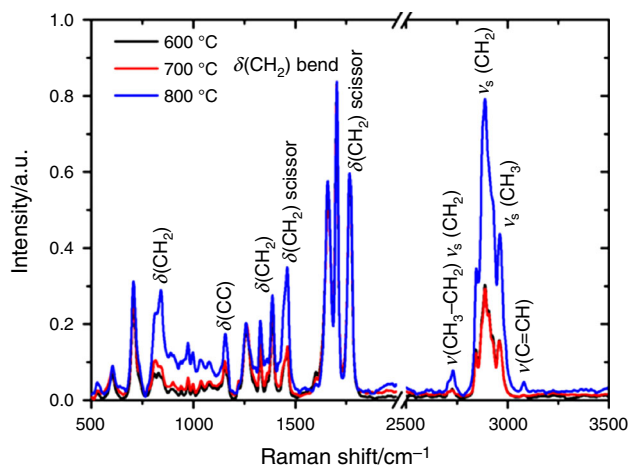

Fig. 3 Normalized Raman spectrum recorded at 20 °C from wax formed by pyrolysis of waste PP at three different temperatures of 600, 700, and 800 °C using Fe as catalyst, for a dwell time of 15 min and in the N_2 atmosphere

which is explained by the generation of –C=C– groups due to radical degradation mechanism.

Thermal analysis (DSC)

Figure 4a shows the heating curves of the 1st DSC cycle of wax formed at different pyrolyzing temperatures. For all the wax samples, a broad endothermic band appears at intermediate temperatures, which can be assigned to wax melting. However, difference in melting behavior can be observed for the different samples. First, the starting and ending temperatures of the melting band transition are different for the different samples. Melting occurs mainly between 30 and 65 °C for wax formed at 600 °C, between 60 and 75 °C for wax formed at 700 °C, between 45 and 65 °C for wax formed at 800 °C. The wax formed at 700 °C shows the highest melting band temperatures as compared to the other samples. Furthermore, the endothermic melting band of the wax formed at 600 °C shows an elongated tail with some minor features on the lower temperature side.

Similarly, noise-like endothermic features also appear to a lower extent for the other samples, especially for the wax formed at 800 °C. All these secondary peaks might be due to a solid-solid transition in the wax crystals, prior to the main melting transition occurring on the right hand side at higher temperatures. Probably, different molar mass fractions existing in the original solid are melting at different temperatures. However, these features are mainly removed after the 1st heating cycle in agreement with the literature [31, 32], as it can be seen in Fig. 4b that shows the heating curves of the second DSC cycle. In Fig 4c, d, the cooling curves of the 1st and 2nd DSC cycles are reported,

Fig. 4 DSC curves of hydrocarbon wax formed by pyrolyzing PP at three different temperatures of 600, 700, and 800 °C using Fe as catalyst, for a dwell time of 15 min and in the N_2 atmosphere: **a** 1st heating scan, **b** 2nd heating scan, **c** 1st cooling scan, **d** 2nd cooling scan
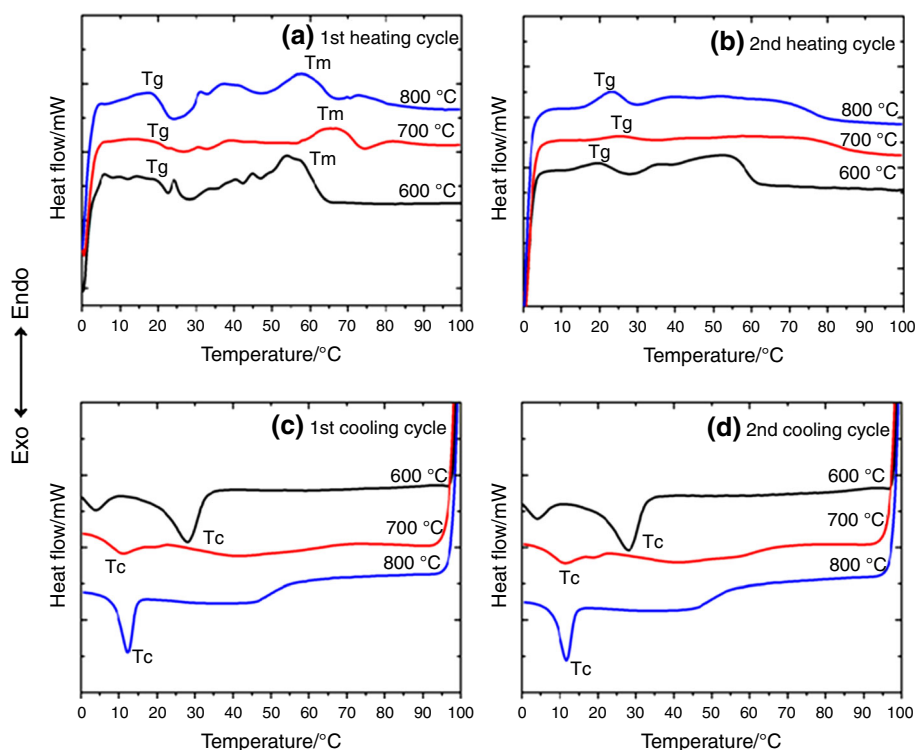
respectively. On cooling, the crystallization behavior of the wax samples can be observed. All the samples show a main exothermic peak associated with solidification. The specific enthalpy of melting of wax is less for wax formed at 700 °C as compared to wax formed at 600 and 800 °C. On cooling, the small features present in the heating curves of the first cycle (Fig. 4a) do not appear, since the wax crystallizes uniformly with the same properties everywhere over the sample. In particular, a common preferential crystal orientation is assumed, and the amorphous parts disappear. This has been confirmed by XRD measurements (Fig. S1), in which the diffraction peaks appear without any change in crystal structure. The overall DSC results in terms of melting band peaks M_p and specific enthalpy values ΔH for both heating and cooling first and second heating cycles are summarized in Table 2.

TG analysis

In Fig. 5, the results of the thermal analysis under N_2 atmosphere for wax formed at different pyrolytic reaction temperature are reported. Figure 5a shows the direct TG curves. For all wax samples, the mass loss appears only above 110 °C, showing that the formed wax was free from moisture. For wax formed at 600 and 800 °C, the mass loss ends at ∼420 °C, whereas for wax formed at 700 °C, the mass loss ends at ∼470 °C, with a steep final decrease in the highest ∼20 °C. The different material degradation

steps can be best pointed out by the differential thermal analysis (DTA) plots, as reported in Fig. 5b. These graphs are the first derivatives of the TG versus the temperature, such that their minima are the points of maximum mass loss and can be assigned as the characteristic (center) temperatures for any given degradation step. As can be seen in Fig. 5b, for the wax formed at 600 °C, degradation occurs in two major steps. The first step proceeds from $T_{onset} \sim 110$ °C up to $T_{end1} \sim 225$ °C and is due to the degradation of low molecular mass alkanes, consistent with our previous observation of the small noise-like endothermic peaks of the respective DSC curve at low temperature (see Fig. 4a). The second step proceeds from T_{end1} up to $T_{end2} \sim 440$ °C. For the wax formed at 800 °C, there is no such clearly defined two-step degradation, but rather a single broad degradation step occurs, which extends up to $T_{end} \sim 470$ °C. In the case of wax formed at 700 °C, the two degradation steps appear, with the first step at approximately the same temperature as the other wax samples, but the second and largely dominating step at much higher temperature, $DTG_{max2} \sim 448$ °C.
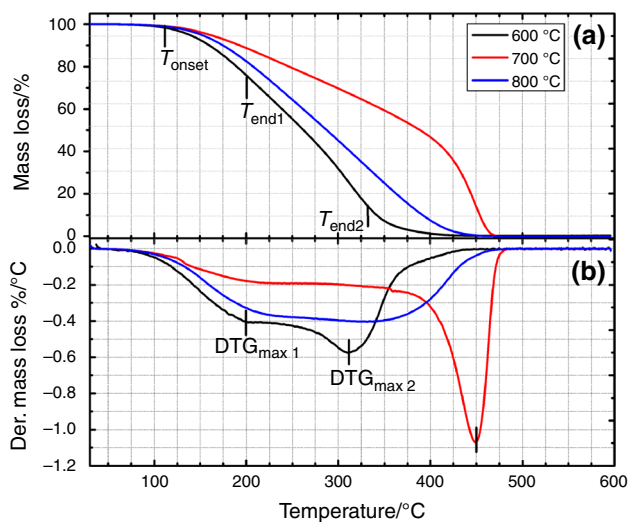
Calorific value of wax

The heating values measured for wax obtained by pyrolysis at 600, 700, and 800 °C are reported in Table 3. These values are generally lower than those for the starting material [27], PP in our case. According to Arabiourrutia

Table 2 Parameters obtained from DSC measurements of wax formed by pyrolysis at three different temperatures of 600, 700, and 800 °C using Fe as catalyst, for a dwell time of 15 min and in the N_2 atmosphere

Pyrolysis Temperature/ °C	Melting point peak position/°C				Specific enthalpy/J kg^{-1}			
	M_p^{1h}	M_p^{2h}	M_p^{1c}	M_p^{2c}	ΔH^{1h}	ΔH^{2h}	ΔH^{1c}	ΔH^{2c}
600	53.8	53.5	28.1	28.1	14.6	12.9	−7.6	−7.6
700	67.0	71.7	41.8	42.1	3.6	10.0	−5.6	−6.1
800	57.8	58.0	33.5	42.5	5.3	11.0	−1.6	−1.3

Superscripts describe the cycle number (1 or 2) and the cycle curve branch ('h' for heating or 'c' for cooling)

Fig. 5 Thermal analysis of wax in N_2 atmosphere: **a** TG and **b** corresponding DTA at three different temperatures of 600, 700, and 800 °C using Fe as catalyst, for a dwell time of 15 min

Table 3 Calorific value of wax prepared at three different temperatures of 600, 700, and 800 °C using Fe as catalyst, for a dwell time of 15 min and in the N_2 atmosphere

Pyrolysis temperature/°C	Calorific value of wax obtained/MJ kg^{-1}
600	42.05
700	43.46
800	45.61

[27], the heating value increases as the temperature increases, irrespective of the material used. The heating value also increases as the chain length, C/H ratio and aromatic concentration increase. The calorific value of soft and hard wax was reported to be ∼44.5 and ∼45 MJ kg^{-1}, respectively [28]. The values corresponding to the waxes obtained here at 600 and 700 °C are lower than those values from the literature, corresponding to fuel oil and petroleum products. The higher heating value of the wax obtained at 800 °C is comparable to that of the original polymer and not much lower than those

corresponding to gasoline or natural gas. Therefore, this kind of wax can be utilized at least as a fuel for its capacity to produce energy.

Conclusions

At low temperature, i.e. 600 °C, all catalysts perform well for PP waste pyrolysis, which gives high yield of wax production of ∼80 mass%. In fact, due to the vigorous gas-solid contact, this reactor may be particularly interesting for selectively obtaining wax. The PP wax obtained has a melting point of ∼70 °C and a calorific value of ∼43 MJ kg^{-1}, which can meet the commercial requirements for fuel applications. These waxes are mainly soft paraffinic, although they are more olefin than the commercial ones. Additionally, when examining the difference among the waxes obtained by pyrolyzing at three different reaction temperatures of 600, 700, and 800 °C, it was found that the wax formed at 700 °C is thermally more stable than those formed at 600 and 800 °C, which can be an advantage for realization of different valuable products from waste PP, such as print ink, shoe or car polishing, and cosmetics. Starting from the working parameters found here, the pyrolysis technique can be useful in commercial perspective for the synthesis of soft wax, also considering that the described experimental setup is cost-effective and allows using waste plastics in any form and in large quantity.

References

1. Alireza B, Gordon M. A review—synthesis of carbon nanotubes from plastic wastes. Chem Eng J. 2012;195–196:377–91.
2. Tschan MJ-L, Brule E, Haquette P, Thomas CM. Synthesis of biodegradable polymers from renewable resources. Polym Chem. 2012;3:836–51.

3. Lin Y, Yen H. Fluidised bed pyrolysis of polypropylene over cracking catalysts for producing hydrocarbons. Polym Degrad Stab. 2005;89:101–8.

4. Siddiqui MN, Redhwi HH. Catalytic coprocessing of waste plastics and petroleum residue into liquid fuel oils. J Anal Appl Pyrolysis. 2009;86:141–7.

5. Mishra N, Das G, Ansaldo A, Genovese A, Malerba M, et al. Pyrolysis of waste polypropylene for the synthesis of carbon nanotubes. J Anal Appl Pyrolysis. 2012;94:91–8.

6. Kaminsky W. Recycling of polymers by pyrolysis. J Phys IV France. 1993;3:1543–52.

7. Mishra N, Pandey S, Patil B, Thakur M, Mewada A, Sharon M, Sharon M. Facile route to generate fuel oil via catalytic pyrolysis of waste polypropylene bags: towards waste management of >20 μm plastic bags. J Fuels. 2014;2014:1–11.

8. Vasile C. Thermal and catalytic decomposition of mixed plastics. J Anal Appl Pyrolysis. 2001;57:287–303.

9. Westerhout RWJ, Waanders J, Kuipers JAM, Van Swaaij WPM. Kinetics of the low-temperature pyrolysis of polyethene, polypropene, and polystyrene modeling, experimental determination, and comparison with literature models and data. Ind Eng Chem Res. 1997;36:1955–64.

10. Bertolini FJ, Gerard E. Value recovery from plastics waste by pyrolysis in molten salts. Conserv Recycl. 1987;10:331–43.

11. Bockhorn H, Hornung A, Hornung U. Mechanisms and kinetics of thermal decomposition of plastics from isothermal and dynamic measurements. J Anal Appl Pyrolysis. 1999;50:77–101.

12. Bockhorn H, Hornung A, Hornung U, Schawaller D. Kinetic study on the thermal degradation of polypropylene and polyethylene. J Anal Appl Pyrolysis. 1999;48:93–109.

13. Bockhorn H, Hornung A, Hornung U. Stepwise pyrolysis for raw material recovery from plastic waste. J Anal Appl Pyrolysis. 1998;46:1–13.

14. Marcilla RA, García-Quesada JC, Sanchez S. Study of the catalytic pyrolysis behaviour of polyethylene—polypropylene mixtures. J Anal Appl Pyrolysis. 2005;74:387–92.

15. Aguado R, Jose JS, Gaisa B. Wax formation in the pyrolysis of polyolefins in a conical spouted bed reactor. Energy. 2002;16:1429–37.

16. Elordi G, Lopez G, Olazar M, Aguado R, Bilbao J. Product distribution modelling in the thermal pyrolysis of high density polyethylene. J Hazard Mater. 2007;144:708–14.

17. Umare PS, Antony R, Gopalakrishnan K, Tembe GL, Trivedi B. Synthesis of low molecular weight polyethylene waxes by a titanium BINOLate-ethylaluminum sesquichloride catalyst system. J Mol Catal A. 2005;242:141–50.

18. Li J, Wang S, Yang X. Study on the conversion technology of waste polyethylene plastic to polyethylene wax. Eng Sourc. 2010;25:77–82.

19. Jagdale P, Sharon M, Kalita G, Maldar NMN, Sharon M. Adv Mater Phys Chem. 2012;2:1–10.

20. Porro SA, Musso S, Giorcelli M, Chiodoni A, Tagliaferro A. Optimization of a thermal-CVD system for carbon nanotube growth. Physica E. 2007;37:16–20.

21. Szabo R, Kiricsi I. Optimization of CCVD synthesis conditions for single-wall carbon nanotubes by statistical design of experiments (DoE). Carbon. 2005;43:2842–9.

22. Kim K, Kim S. Nickel particles prepared from nickel nitrate with and without urea by spray pyrolysis. Powder Technol. 2004;145:155–62.

23. Arandes M, Torre I, Castan P, Olazar M, Bilbao J, Paı U. Catalytic cracking of waxes produced by the fast pyrolysis of polyolefins. Energ Fuel. 2007;21:579–87.

24. Sharratt PN, Lin Y. Investigation of the catalytic pyrolysis of high-density polyethylene over a HZSM-5 catalyst in a laboratory fluidized-bed reactor. Ind Eng Chem Res. 1997;36:5118–24.

25. Park DW, Hwang EY, Kim JR, Choi JK, Kim YA, Woo HC. Catalytic degradation of polyethylene over solid acid catalysts. Polym Degrad Stab. 1999;65:3–8.

26. Kiran Ciliz N, Ekinci E, Snape CE. Pyrolysis of virgin and waste polypropylene and its mixtures with waste polyethylene and polystyrene. Waste Manage. 2004;24:173–81.

27. Arabiourrutia M, Elordi G, Lopez G, Borsella E, Bilbao J, Olazar M. Characterization of the waxes obtained by the pyrolysis of polyolefin plastics in a conical spouted bed reactor. J Anal Appl Pyrolysis. 2012;94:230–7.

28. Chaala A, Darmstadt H, Roy C. Vacuum pyrolysis of electric cable wastes. J. Anal Appl Pyrolysis. 1997;39:79–96.

29. Faolain EO, Hunter MB, Byrne JM, Kelehan P, Lambkin HA, Byrne HJ, et al. Raman spectroscopic evaluation of efficacy of current paraffin wax section dewaxing agents. J Histochem Cytochem. 2005;53:121–9.

30. Zheng M, Du W. Phase behavior, conformations, thermodynamic properties, and molecular motion of multicomponent paraffin waxes: a Raman spectroscopy study. Vib Spectrosc. 2006;40:219–24.

31. Krupa I, Luyt AS. Thermal properties of uncross-linked and cross-linked LLDPE/wax blends. Polym Degrad Stab. 2000;70:111–7.

32. Krupa I, Luyt AS. Thermal properties of polypropylene/wax blends. Thermochim Acta. 2001;372:137–41.